Pergamon

Tetrahedron 54 (1998) 15739–15758

TETRAHEDRON

Circular dichroism studies of bisindole *Vinca* alkaloids[1]

Craig A. Parish[a], Jian-Guo Dong[a], William G. Bornmann[b], Joan Chang[a], Koji Nakanishi[a]* and Nina Berova[a]*

[a]Department of Chemistry, Columbia University, New York, NY 10027, USA
[b]Memorial Sloan-Kettering Cancer Center, New York, NY 10021, USA

Received 24 August 1998; accepted 20 October 1998

Abstract: The analysis of a series of seventeen vinblastine analogs by circular dichroism is described. Exciton coupling of the indole and indoline chromophores of these compounds provides a general, non-empirical method for the assignment of the C16' configuration with the bioactive C16'-S and the inactive C16'-R analogs giving rise, respectively, to positive and negative couplets. An analysis of the non-coupled transitions of the CDs indicates that a positive Cotton effect at 305 nm, although empirical, is associated with bioactivity. Theoretical calculations of the UV and CD spectra of vinblastine diastereomers are also described.

Keywords: circular dichroism, electronic spectra, alkaloids, theoretical studies.

INTRODUCTION

The *Vinca* alkaloids vinblastine (**1**) and vincristine (**2**), initially isolated independently by Noble and Svoboda from *Catharanthus roseus*,[1,2] are clinically important cancer chemotherapeutics. Because of the wide range of activity of these drugs against numerous cancer types, including Hodgkin's and non-Hodgkin's lymphomas, acute lymphoblastic leukemia, breast carcinoma, Wilms' tumor, and Ewing's sarcoma, vinblastine and vincristine continue to play a prominent role in cancer treatments. Mechanistic studies of these drugs indicate that they bind to tubulin, the heterodimeric building block for microtubule polymerization, and that by interfering with microtubule formation, they lead to mitotic arrest and eventually to cell death, i.e., cell division is inhibited and tumor growth is slowed. The binding of the *Vinca* alkaloids to tubulin disrupts the normal polymerization of the tubulin heterodimer into elongated microtubules and this binding site is discrete from that of other tubulin

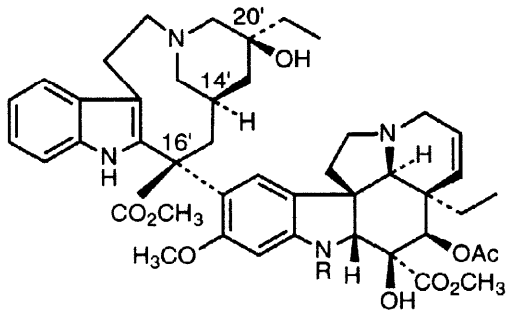

1 vinblastine (VBL), R = CH_3
2 vincristine (VCR), R = CHO

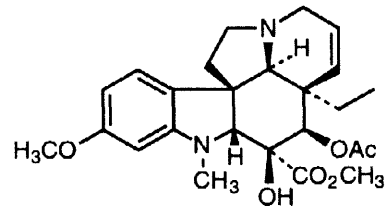

3 vindoline (VDL)

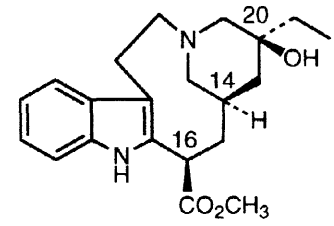

4 cleavamine

[1] Dedicated to Professor Ian Scott on the occasion of his 70th birthday.

0040-4020/98/$ - see front matter
PII: S0040-4020(98)00988-0

binding agents such as paclitaxel or colchicine.[3-6]

The *Vinca* alkaloids, or bisindole alkaloids, consist of two core ring systems which contain the indole and indoline chromophores. Vinblastine (**1**) is comprised of two moieties; the lower half (as drawn), vindoline (**3**), which contains the N-methyl-indoline chromophore, and the upper half, cleavamine **4**, which contains an indole chromophore and is linked to vindoline (**3**) through the cleavamine C16 (C16' of vinblastine) stereocenter. The absolute stereochemistry of vinblastine and vincristine was originally established by X-ray crystallography.[7] ^{13}C NMR spectroscopy has also been used to determine the configuration of the C16' stereocenter.[8,9] Total chemical synthesis has provided routes for the preparation of numerous vinblastine analogs.[10-14] Structure activity studies have demonstrated that the C16' configuration is critical for bioactivity, i.e., the natural 16'-S configuration is required and inversion of configuration at C16' results in an analog which cannot bind to the protein.[14] Similarly, vinblastine function is sensitive to the C14' configuration since inversion of this center also leads to a loss of activity.[14] Modifications at the C20' stereocenter have also led to alterations of *Vinca* alkaloid activity.[15,16]

Circular dichroism (CD) can be used to analyze vinblastine and its analogs by correlating the stereochemistry of these compounds with the sign of certain CD Cotton effects (CEs) (see Figure 3 below). Kutney, Scott and coworkers initially demonstrated that CD could be used for the interpretation of the vinblastine C16' stereochemistry.[17] Recently, we have confirmed the validity of this method by a preliminary theoretical analysis of the CD of vinblastine.[18] The interaction of the electric transition moments of the indole and indoline chromophores lead to CD bands which can be directly related to molecular configuration and conformation. Potier and coworkers have indicated that C16' stereochemistry could be determined from the sign of the Cotton effect (CE) of vinblastine-type compounds at ~255 nm.[10,19] However, we have shown that the intense bisignate curve at 228 nm and 214 nm in vinblastine CD arises from exciton coupling of the indole ^1B_b and indoline ^1B_b transitions[20,21] (see Figure 8 below) and the sign of the couplet is directly related to the C16'-configuration.[18] Here, the preparation and CD analysis of an extensive series of vinblastine analogs, especially the complementary set of diastereomers at C16', C14' and C20' of the cleavamine portion of vinblastine, has confirmed the validity of using the sign of the exciton couplet to determine the C16' configuration. This set of compounds further allow for the analysis of other non-coupled CD bands observed at 255 and 305 nm. Additional theoretical derivation of the CD of vinblastine analogs has shown the utility of CD for obtaining conformational information.

RESULTS AND DISCUSSION

Synthesis.

Chemical synthesis is providing an increasing number of vinblastine analogs which allow for an increased understanding of the molecular requirements for bioactivity as well as for extensive conformational and spectroscopic analysis.[11-13] Vinblastine (**1**) is composed of two half molecules, vindoline (**3**) and cleavamine **4**, which are attached via the C16' stereocenter of the cleavamine moiety. The preparation of all eight diastereomers

Vinblastine Diastereomers

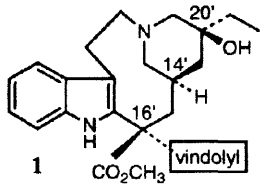

vinblastine
14'-R, 16'-S, 20'-S

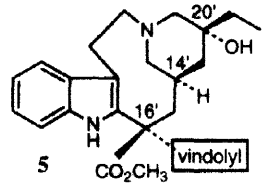

leurosidine
14'-R, 16'-S, 20'-R

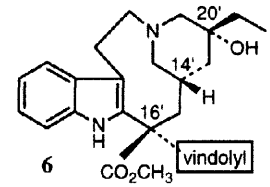

14'-S, 16'-S, 20'-R

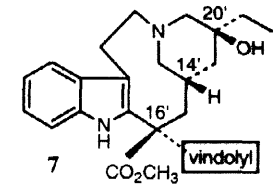

14'-S, 16'-S, 20'-S

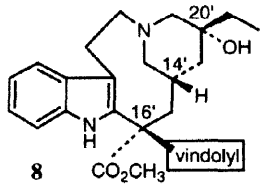

vincovaline
14'-S, 16'-R, 20'-R

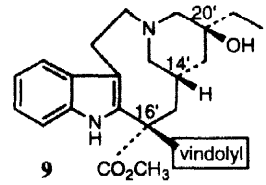

20'-epi-vincovaline
14'-S, 16'-R, 20'-S

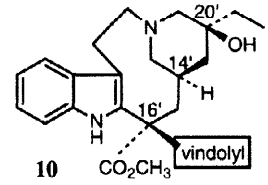

14'-R, 16'-R, 20'-S

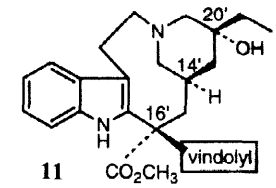

14'-R, 16'-R, 20'-R

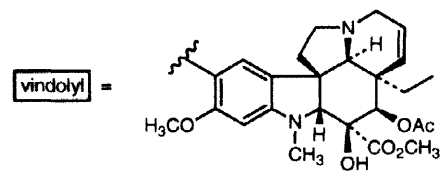

Cleavamine Diastereomers

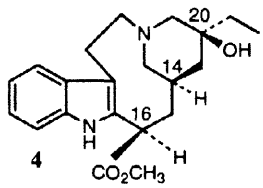

14-R, 16-S, 20-S

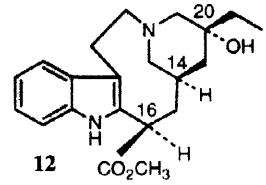

14-R, 16-S, 20-R

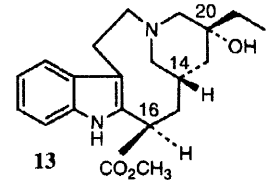

14-S, 16-S, 20-R

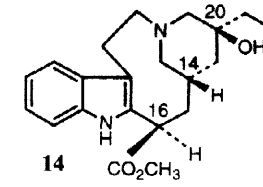

14-S, 16-S, 20-S

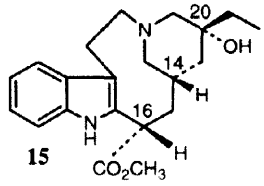

14-S, 16-R, 20-R

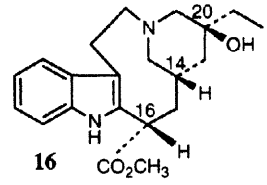

14-S, 16-R, 20-S

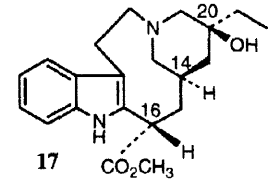

14-R, 16-R, 20-S

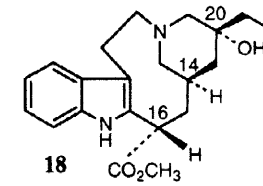

14-R, 16-R, 20-R

Scheme 1.

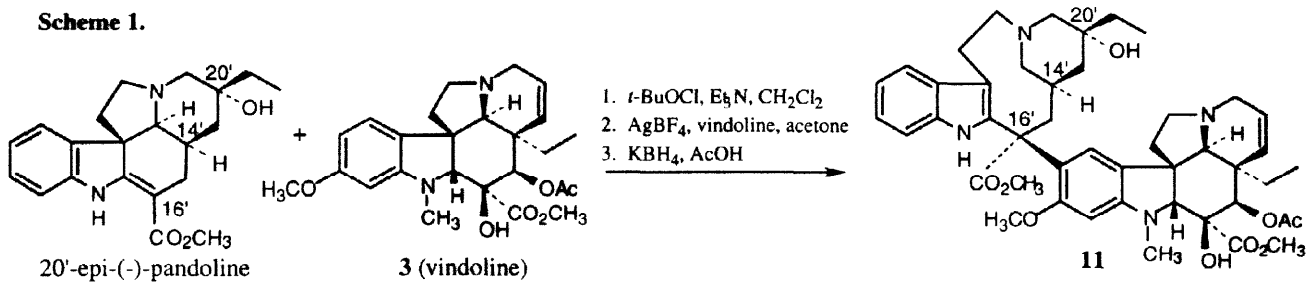

of vinblastine at positions C14'-C16'-C20' of the cleavamine half have been accomplished and a comparison of the circular dichroic spectra of this entire series has been studied for the first time. The syntheses of vinblastine (**1**), leurosidine (**5**), vincovaline (**8**) and 20'-epi-vincovaline (**9**) were accomplished according to literature procedures.[12] The methodology involved in these preparations can be extended for the structure-activity studies of additional vinblastine derivatives. The coupling of four pandoline diastereomers ((+)-pandoline, (-)-pandoline, 20'-epi-(+)-pandoline and 20'-epi-(-) pandoline)[22] with vindoline (**3**) (e.g., see Scheme 1) via a chloroimine intermediate provided vinblastine diastereomers **6-7** and **10-11**. The absolute configuration of these analogs was established through their synthesis from chiral precursors with known absolute configuration and further confirmed by NMR spectroscopy.[12] The series of cleavamine diastereomers which comprise the upper half of vinblastine (16α- and 16β-(carbomethoxy)-velbanamines, more commonly referred to as cleavamines, (**4** and **13-18**) were also prepared according to literature procedures[8,9,22-25] so that the two chromophores of vinblastine could be independently studied by spectroscopic means. Cleavamine **12** was not prepared for analysis in this work. The spiro (**23-24**) and seven-membered ring (**25-26**) vinblastine analogs were prepared following procedures analogous to those already present in the literature[12] and will be described in greater detail in a future publication.

UV/CD of vindoline and cleavamine.

The spectroscopic data of the separate "half-molecules" were measured in order to clarify the interpretation of the CD of vinblastine (**1**) and analogs **5-11**. Vinblastine and its diastereomers **5-11** contain identical vindolyl moieties as the indoline chromophore:

Vindoline (**3**): The UV of vindoline in acetonitrile (Figure 1) displays three peaks corresponding to the ^1B_b (213 nm), ^1L_a (253 nm) and ^1L_b (305 nm) transitions (see theoretical studies in this work),[17] which correlate well with the CD Cotton effects (Figure 1, Table 1). The strongest CE is derived from the ^1B_b transition and appears at 217 nm ($\Delta\varepsilon$ = -18.2).

Cleavamines **4**, **12-18**: The vinblastine diastereomers (**1**, **5-11**) differ in the stereochemistry of the cleavamine half of the molecule. These diastereomers are derived from all eight possible combinations of the three stereogenic centers at C14, 16 and 20 of (carbomethoxy)-velbanamine. The UV of the seven available diastereomers

Table 1.
UV/CD Data for vindoline (**3**) and cleavamine **4** analogs.[a)]

Compound	Configuration[b)] *14*-16-20		UV: ε (× 10^{-3} M^{-1}•cm^{-1}) CD: Δε (M^{-1}•cm^{-1})
3 (VDL)	-	*UV*	213 (31.7), 253 (7.2), 305 (5.0)
		CD	217 (-18.2), 232 (+6.1), 254 (+13.7), 318 (+1.0)
4	*R* - S - S	*UV*	200 (22.6), 226 (28.8), 285 (7.4)
		CD	199 (+16.8), 234 (-27.6), *290 (+1.3)*
12	*R* - S - R	*UV*	NA[c)]
		CD	NA
13	*S* - S - R	*UV*	200 (23.9), 227 (31.3), 285 (7.8)
		CD	209 (+8.2), 234 (-16.0), *280 (-2.9)*
14	*S* - S - S	*UV*	200 (24.2), 227 (31.2), 284 (8.0)
		CD	210 (+7.3), 232 (-18.4), *279 (-2.3)*
15	*S* - R - R	*UV*	200 (24.5), 226 (29.1), 284 (7.6)
		CD	197 (-14.6), 234 (+24.1), *294 (-1.4)*
16	*S* - R - S	*UV*	201 (24.9), 226 (29.1), 285 (7.2)
		CD	200 (-13.1), 235 (+21.1), *292 (-1.1)*
17	*R* - R - S	*UV*	200 (23.8), 227 (31.2), 285 (7.7)
		CD	210 (-9.0), 234 (+16.3), *276 (+2.7)*
18	*R* - R - R	*UV*	200 (26.5), 227 (31.2), 285 (8.0)
		CD	210 (-6.6), 233 (+17.3), *279 (+2.1)*

a) All UV and CD spectra were recorded in acetonitrile.
b) Absolute configurations of cleavamine diastereomers have been established.[9,22,23,25] C14 configurations and the long wavelength CEs are indicated in italics.
c) Not available; cleavamine **12** is not reported in this study.

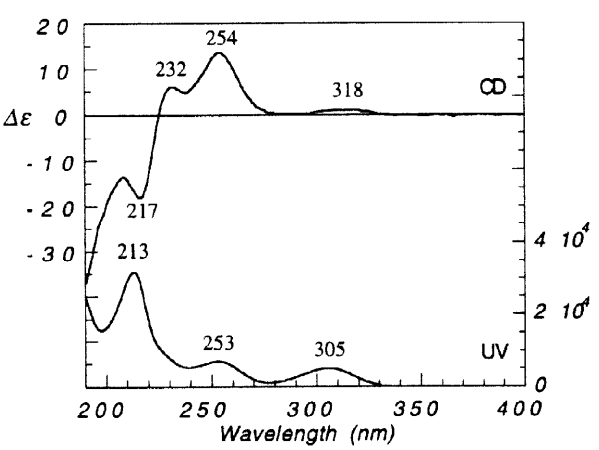

Figure 1. CD and UV Spectra of Vindoline (**3**) in acetonitrile.

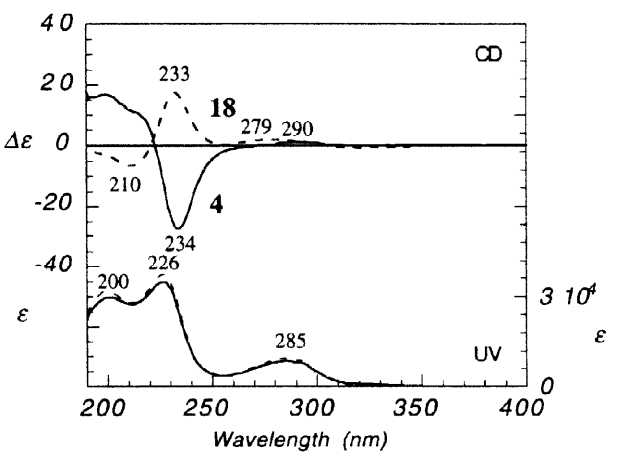

Figure 2. CD and UV Spectra of Cleavamine **4** (solid line) and Cleavamine **18** (dashed line) in acetonitrile.

contain peaks corresponding to the ^1B_b (227 nm) transition as well as overlapping ^1L_a and ^1L_b transitions around 285 nm;[17] these transitions are all related to the indole chromophore of each cleavamine (a theoretical calculation of the direction of these transitions is shown in Figure 8). In the CD spectra, the ^1B_b transition leads to the strongest CE at 232-235 nm. The CD and UV for two cleavamine diastereomers, **4** and **18**, are shown in Figure 2. Although no empirical correlation exists between the CE signs of the 232-235 nm and 197-210 nm CD bands, the weak CE at 276-294 nm can be correlated with the C14 stereochemistry in that all C14-S diastereomers (β 14'-H as drawn) have a negative band and *vice versa* (Table 1).

UV/CD of vinblastine diastereomers.

While the UV of vinblastine analogs correspond to a summation of the two "half-molecules", a dramatic change in the CD of vinblastine (**1**) is observed as compared to that of the isolated chromophores. For vinblastine (**1**), an intense bisignate curve arising from coupling of the ^1B_b transitions of the indole and indoline halves is seen at 228 nm/214 nm (Δε = +31.0 / -73.4) (Figure 3). All vinblastine epimers (**5**-**11**) display similar exciton couplets in this region. The UV and CD of vincovaline (**8**), the diastereomer of vinblastine with opposite configuration at 14', 16', and 20' are also shown in Figure 3. Table 2 lists data for all eight diastereomers of vinblastine as well as that for vincristine.

Stereochemistry at C16': Reflecting the C16' stereochemistry, the signs of the couplets are positive for four diastereomers and negative for the remaining four (Table 2); since C16' is the stereocenter which links the two "half-molecules", it is this configuration which determines the sign of the bisignate curve. Calculations of the CD of vinblastine have closely reproduced the experimental data[18] and this theoretical analysis of vinblastine conformation has been extended in this paper to other vinblastine diastereomers (see below). The bisignate curve for vincristine (**2**) (A = +37.5), where the N-methyl-indoline of vinblastine is replaced by an N-formyl-indoline,

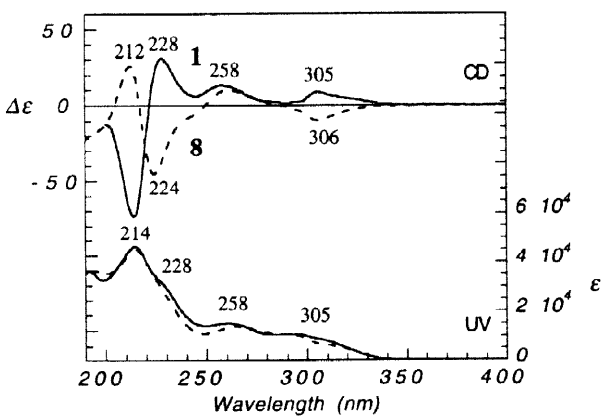

Figure 3. CD and UV spectra of VBL (**1**) (solid line) and Vincovaline (**8**) (dashed line) in acetonitrile.

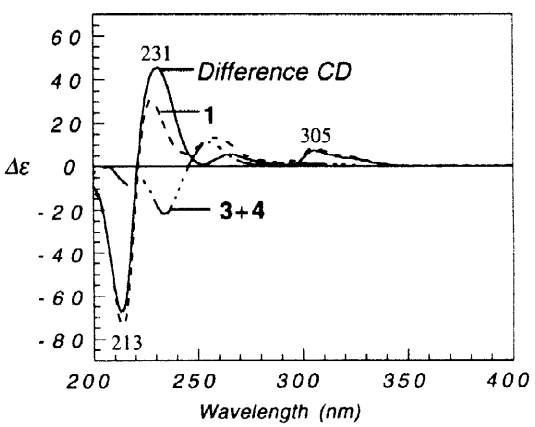

Figure 4. Vinblastine (**1**) difference CD spectrum.

Table 2.
UV/CD Data for Vinblastine Analogs.[a]

Compound	Configuration[b] 14'-16'-20'		UV: ε (× 10^{-3} M^{-1}•cm^{-1}) CD: Δε (M^{-1}•cm^{-1})	$A_{214/228}$[c]
1 (VBL)	*R* - **S** - S	*UV*	214 (46.2), 260 (15.1), 296 (10.6)	
		CD	**214 (-73.4), 228 (+31.0)**, 258 (+13.6), *305 (+9.0)*	**+104.4**
		CD 3 + 4	218 (-8.6), 234 (-22.0), 255 (+11.5), 295 (+1.5)	
		Difference CD	**213 (-67.4), 231 (+45.7)**, 265 (+5.9), *305 (+7.8)*	**+113.1**
2 (VCR)	*R* - **S** - S	*UV*	198 (41.6), 222 (29.5), 298 (8.8)	
		CD	**207 (-24.5), 234 (+13.0)**, 253 (+10.3), *303 (+7.3)*	**+37.5**
5 (Leurosidine)	*R* - **S** - R	*UV*	215 (45.1), 265 (13.6), 287 (10.7), 295 (9.1)	
		CD	**214 (-67.2), 227 (+32.9)**, 261 (+15.0), *306 (+7.3)*	**+100.1**
6	*S* - **S** - R	*UV*	194 (33.8), 217 (45.2), 265 (14.2), 295 (11.3)	
		CD	**212 (-61.7), 227 (+43.5)**, 262 (+39.3), *314 (-13.9)*	**+105.2**
		CD 3 + 13	217 (-12.8), 235 (-10.4), 254 (+13.0), 283 (-2.7), 319 (+1.0)	
		Difference CD	**211 (-54.2), 227 (+48.4)**, 265 (+33.5), *315 (-14.7)*	**+102.6**
7	*S* - **S** - S	*UV*	195 (34.9), 217 (45.1), 265 (13.2), 295 (11.5)	
		CD	**212 (-61.7), 227 (+47.3)**, 262 (+36.8), *313 (-13.4)*	**+109.0**
		CD 3 + 14	217 (-13.7), 233 (-12.3), 254 (+13.2), 283 (-2.0), 318 (+1.5)	
		Difference CD	**211 (-53.2), 227 (+57.1)**, 264 (+30.6), *314 (-14.6)*	**+110.3**
8 (Vincovaline)	*S* - **R** - R	*UV*	214 (48.7), 256 (14.8), 290 (10.6), 297 (10.9)	
		CD	**212 (+26.1), 224 (-44.8)**, 259 (+10.0), *306 (-9.9)*	**-70.9**
		CD 3 + 15	217 (-12.8), 235 (-10.4), 254 (+13.0), 283 (-2.7), 318 (+1.0)	
		Difference CD	**213 (+34.6), 225 (-39.1)**, 270 (+7.3), *306 (-9.8)*	**-73.7**
9 (20'-epi-Vincovaline)	*S* - **R** - S	*UV*	214 (48.6), 258 (14.5), 289 (11.1), 294 (11.0)	
		CD	**212 (+21.5), 224 (-43.2)**, 263 (+4.92), *304 (-7.7)*	**-64.7**
		CD 3 + 16	216 (-26.8), 235 (+26.5), 250 (+17.4), 292 (-1.1), 318 (+1.7)	
		Difference CD	**212 (+46.6), 228 (-49.2)**, 276 (+1.2), *305 (-8.1)*	**-95.8**
10	*R* - **R** - S	*UV*	216 (51.4), 264 (15.4), 296 (12.5)	
		CD	**211 (+21.9), 225 (-41.8)**, 263 (-20.7), *313 (+9.9)*	**-63.7**
		CD 3 + 17	215 (-25.2), 233 (+22.1), 252 (+13.9), 287 (+2.5), 301 (+2.0)	
		Difference CD	**212 (+45.9), 228 (-52.3)**, 258 (-31.1), *313 (+9.2)*	**-98.2**
11	*R* - **R** - R	*UV*	218 (50.4), 267 (13.9), 288 (12.7), 295 (12.7)	
		CD	**211 (+25.9), 225 (-54.9)**, 262 (-22.3), *312 (+11.3)*	**-81.0**
		CD 3 + 18	215 (-23.3), 232 (+23.4), 254 (+14.0), 287 (+1.8), 301 (+1.2)	
		Difference CD	**212 (+48.0), 227 (-67.1)**, 259 (-32.7), *313 (+10.9)*	**-115.1**

a) All UV and CD spectra were recorded in acetonitrile.
b) Absolute configuration has been established by total chemical synthesis and NMR: **1, 5, 8, 9**;[12] **6-7, 10-11**, this reference. Vincristine is commercially available. Data in bold indicate the C16' stereochemistry and the exciton coupled CEs. C14' configurations and the long wavelength CEs are indicated in italics.
c) A = Δε(~228 nm) - Δε(~214 nm).

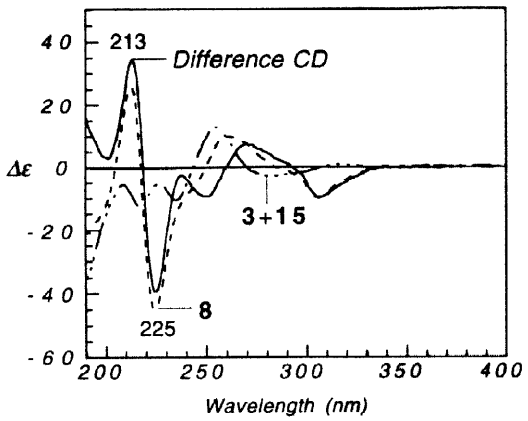

Figure 5. Vincovaline (**8**) difference CD spectrum.

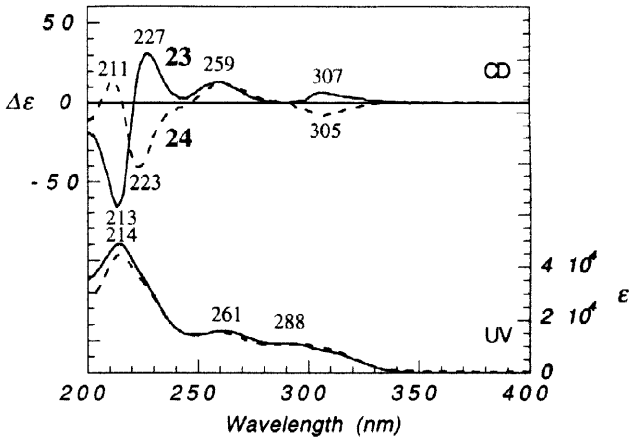

Figure 6. CD and UV spectra of analogs **23** (solid line) and **24** (dashed line) in acetonitrile.

is still positive, although weaker than the exciton couplet observed for vinblastine, presumably owing to the conversion of the aromatic amino function to an amide function.

Difference CD: A more accurate evaluation of the intensity of the bisignate CD curve arising from exciton coupling between the indole and indoline halves is gained by subtracting the CD contributions due to the inherent chirality of the two isolated chromophoric halves from the overall CD (Table 1). As demonstrated for vinblastine (**1**) and vincovaline (**8**) in Figures 4 and 5, subtraction of the sum of the two half-molecules (**3** (vindoline) + cleavamine **4** for vinblastine (**1**); and **3** (vindoline) + cleavamine **15** for vincovaline (**8**)) yields the difference CD. In general, the difference CDs with bands at 228 and 214 nm are more symmetric than the original experimental curves. For analogs with the 16'-S configuration, the A values for the experimental and difference CDs were very similar (Table 2). However, the A values for 16'-R diastereomers were increased more dramatically, especially with vinblastine analogs **9**, **10** and **11** (Table 2). This subtraction led to amplitudes of the coupling of ca. ± 100 for all vinblastine diastereomers except for analog **8** ($\Delta\Delta\varepsilon$ (difference CD) = -73.7) (Figure 5). Since the difference CD contains other CEs in addition to the bisignate curve, it is apparent that either the new environment in which the indole or indoline chromophores are placed lead to new non-coupled Cotton effects, or that other weaker coupling of indole and indoline transitions is occurring.

CD Cotton effects above 240 nm: In addition to the exciton couplet, two additional CEs are present in the CD spectra of vinblastine analogs. The CEs at 258 nm is derived from the indoline ^1L_a transition while the band at 305 nm is due to overlapping ^1L_a and ^1L_b transitions of indole as well as the ^1L_b transition of indoline (see Figure 8). In vindoline (**3**) alone, these CEs are relatively weak, especially above 300 nm ($\Delta\varepsilon$(318 nm) = +1.0) (Table 1). In vinblastine (**1**) (see Table 2, Figure 3), the amplitude of the 254 nm band ($\Delta\varepsilon$(258 nm) = +13.6) is quite similar in intensity to that found in vindoline ($\Delta\varepsilon$(254 nm) = +13.7) However, in other isomers such as analogs **10** and **11**, this band becomes strongly negative (Table 2) (**10**: $\Delta\varepsilon$(263 nm) = -20.7; **11**: $\Delta\varepsilon$(262 nm) = -22.3. Comparison of the varying CEs observed in both the experimental and difference CD spectra led to no clear cut correlation between this CE and vinblastine stereochemistry; thus, a combination of local environmental effects must be

influencing this band. It is clear that that C16' stereochemistry does not correlate with the sign of the CE at 255 nm as has previously been reported;[10,19] this relationship does not hold over the wider range of vinblastine analogs studied here.

In contrast, the longer wavelength CE of vinblastine (**1**) around 305 nm has a more apparent stereochemical significance. The CD spectra of cleavamines **4** and **13-18** contain a CE at 276-294 nm (indole ^1L_a and ^1L_b transitions, $\Delta\varepsilon = \pm 1$-3), the sign of which can be directly correlated to the stereochemistry at C14. This weak band is positive for C14-R and negative for C14-S (Table 1, see italics). While the strong exciton couplets allow for the analysis of C16'-stereochemistry, the weak ^1L_a and ^1L_b transitions are more difficult to interpret. It is less clear which transition is most responsible for the 305 nm CE of vinblastine. The attachment of vindoline (**3**) to cleavamines **4** and **13-18** results in the intensification of this CE around 305 nm, i.e., 303-313 nm ($\Delta\varepsilon = \pm 7$-14) (Table 2, see italics). This is presumably due to the amplification of the chiral environment of the indole chromophore by attachment of the vindoline moiety, which alters the influence on the indole transition. Again, this CE is positive for C14'-R while it is negative for C14'-S (see Table 2). This analysis provides an empirical method for the assignment of the C14' configuration. No significance on the shape of the CD spectrum can be attributed to C20'.

UV/CD of Vinblastine Structural Analogs.

While the CD of vinblastine diastereomers provided consistent results in terms of the exciton couplet at 228 nm/214 nm (C16' stereochemistry) and the ~305 nm Cotton effect (C14' stereochemistry), it was of interest to determine whether additional vinblastine analogs which differ more significantly in structure from the native molecule might also share these spectroscopic characteristics. The analysis here centered on three groups of

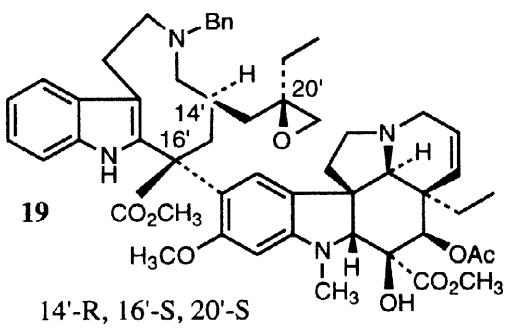

14'-R, 16'-S, 20'-S

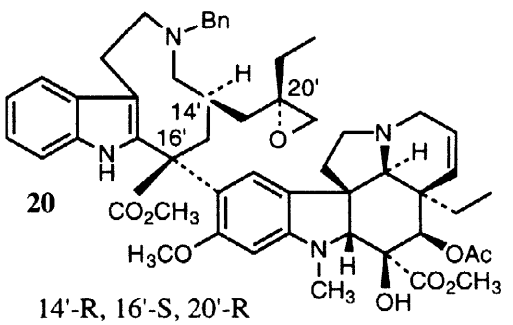

14'-R, 16'-S, 20'-R

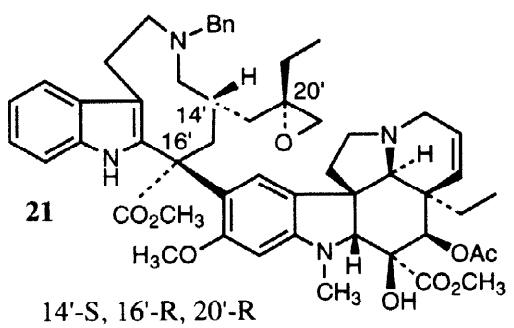

14'-S, 16'-R, 20'-R

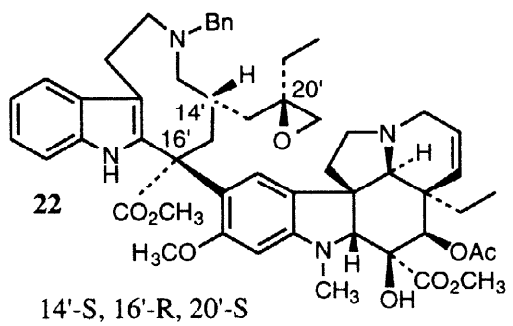

14'-S, 16'-R, 20'-S

analogs: epoxides **19-22**, spiro analogs **23** and **24**, and seven membered ring compounds **25** and **26**. The calculation of difference CDs for these compounds was not possible since none of the appropriate cleavamine "half-molecules" were prepared.

Epoxides **19-22** (Table 3): These compounds can be converted to vinblastine and three of its diastereomers by debenzylation and subsequent epoxide opening. While these analogs do not have the vinblastine core structure, the shape of the CD spectrum of each was quite similar to that of the intact molecule. The sign of the exciton couplet was consistent with the fact that C16'-S analogs give positive A values and C16'-R result in negative coupling. The amplitude of the couplet was similar to that of the vinblastine diastereomers (cf. Tables 2 and 3) indicating that the solution structure of these compounds are quite similar to vinblastine itself in terms of the relative orientation of the two chromophores. The sign of the ~305 nm band also agrees with the observation described above which implicates C14' stereochemistry as a direct influence on the sign of this Cotton effect.

Spiro analogs **23** and **24** (Table 3): The results with these compounds are similarly consistent with the previously discussed analysis of the CD (Figure 6, Table 3). Spiro vinblastine **23** is C16'-S and has a positive A value ($\Delta\Delta\varepsilon$ = +97.0). It is also C14'-R, indicating that the CE at ~305 nm should be positive ($\Delta\varepsilon$(307 nm) = +6.7). Analog **24** is C16'-R and has a negative A value ($\Delta\Delta\varepsilon$ = -54.7). It is also C14'-S, indicating that the CE at ~305 nm should be negative ($\Delta\varepsilon$(305 nm) = -7.8), as is observed.

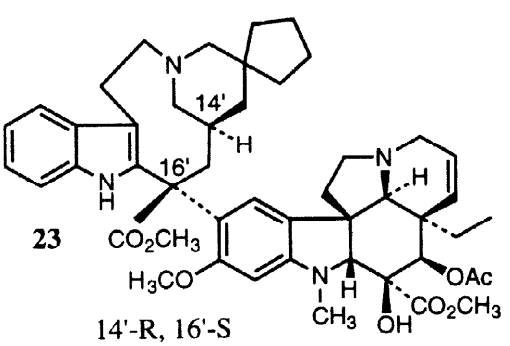

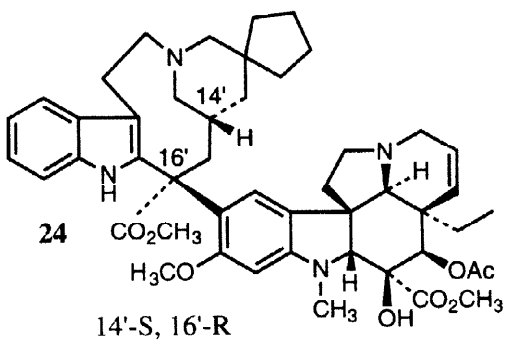

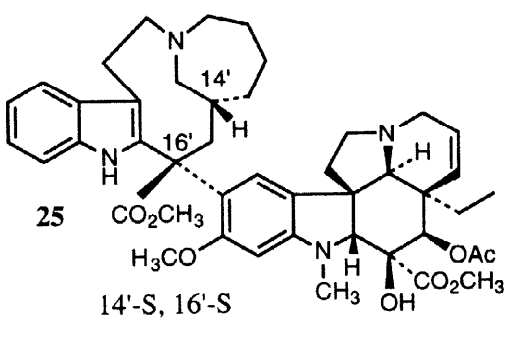

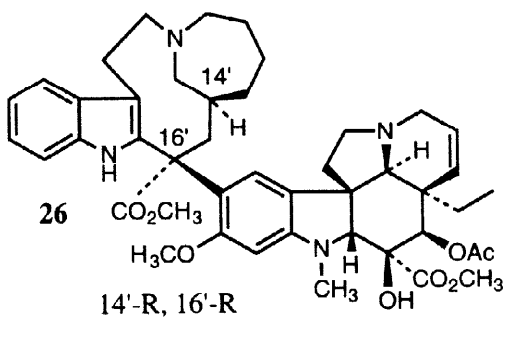

Table 3.
UV/CD Data for Vinblastine Analogs.[a]

Cmpd	Configuration[b] 14'-16'-20'		UV: ε (× 10^{-3} M^{-1}•cm^{-1}) CD: Δε (M^{-1}•cm^{-1})	$A_{212/225}$[d]
19	*R* - **S** - S	*UV*	193 (59.7), 214 (52.4), 264 (15.0), 289 (13.0)	
		CD	204 (-34.5), **214 (-63.1)**, **226 (+28.6)**, 258 (+20.9), *303 (+8.0)*, 318 (+7.0)	**+91.7**
20	*R* - **S** - R	*UV*	193 (60.2), 214 (51.4), 264 (15.0)	
		CD	200 (-36.2), **213 (-62.4)**, **227 (+24.4)**, 259 (+20.7), *305 (+7.0)*, 318 (+7.0)	**+86.8**
21	*S* - **R** - R	*UV*	192 (59.0), 214 (56.7), 260 (15.0), 290 (13.3)	
		CD	194 (-20.1), **211 (+8.4)**, **223 (-71.0)**, 262 (+7.8), *304 (-10.3)*	**-79.4**
22	*S* - **R** - S	*UV*	192 (60.5), 214 (56.1), 258 (14.9), 290 (13.1)	
		CD	**210 (+7.9)**, **223 (-69.5)**, 263 (+6.3), *304 (-9.7)*	**-77.4**
23	*R* - **S** - NA[c]	*UV*	214 (48.9), 261 (15.9), 288 (11.2)	
		CD	**213 (-65.8)**, **227 (+31.2)**, 259 (+13.5), *307 (+6.7)*	**+97.0**
24	*S* - **R** - NA	*UV*	215 (44.8), 259 (15.4), 295 (11.2)	
		CD	**211 (+14.5)**, **223 (-40.2)**, 262 (+12.6), *305 (-7.8)*	**-54.7**
25	*S* - **S** - NA	*UV*	215 (50.3), 260 (14.2), 291 (11.2)	
		CD	**214 (-63.1)**, **228 (+43.5)**, 256 (+14.3), *304 (+3.1)*, 324 (+2.2)	**+106.6**
26	*R* - **R** - NA	*UV*	214 (47.9), 256 (13.7), 295 (11.8)	
		CD	**211 (+16.1)**, **223 (-51.8)**, 259 (+8.0), *303 (-8.6)*	**-70.0**

a) All UV and CD spectra were recorded in acetonitrile.
b) Absolute configuration has been established by total chemical synthesis and NMR: **19-22**;[12] **23-26**, unpublished data. Data in bold indicate the C16' stereochemistry and the exciton coupled CEs. C14' configurations and the long wavelength CEs are indicated in italics.
c) Not applicable.
d) A = Δε(~225 nm) - Δε(~212 nm).

Table 4.
Calculated CD and UV Spectra for Vinblastine Analogs, Vindoline and Cleavamine.[a]

Compound	Configuration[b] 14'-16'-20'		UV: ε (× 10^{-3} M^{-1}•cm^{-1}) CD: Δε (M^{-1}•cm^{-1})	**A (calc)**[c]
1 (VBL)	R - **S** - S	*UV*	216 (63.3), 249 (21.7), 301 (5.5)	
		CD	**210 (-47.3)**, **227 (+17.6)**, 249 (+8.7), 289 (+1.8)	**+64.9**
3 (VDL)		*UV*	216 (44.2), 254 (16.6), 313 (0.74)	
4	R - S - S	*UV*	224 (40.6), 298 (3.8)	
7	S - **S** - S	*UV*	216 (61.9), 249 (23.9), 313 (7.3)	
		CD	**212 (-33.8)**, **229 (+23.8)**, 314 (+3.0)	**+57.6**
10	R - **R** - R	*UV*	218 (66.5), 248 (20.9), 310 (7.1)	
		CD	**213 (+38.7)**, **229 (-36.7)**, 296 (-2.8)	**-75.4**
11	R - **R** - S	*UV*	217 (63.5), 250 (22.2), 298 (5.5)	
		CD	**210 (+21.7)**, **226 (-26.9)**, 291 (-3.1)	**-48.6**

a) Theoretical calculations were performed as described in the text.
b) Data in bold indicate the C16' stereochemistry and the exciton coupled CEs.
c) A = Δε(~228 nm) - Δε(~212 nm).

Seven-membered ring compounds **25** and **26** (Table 3): While **25** is C16'-S and has a positive exciton couplet ($\Delta\Delta\varepsilon$ = +106.6), analog **26** is C16'-R and is negative ($\Delta\Delta\varepsilon$ = -70.0)(Table 3). These two compounds are the only examples where the correlation of the CE sign at ~305 nm differs from the other analogs studied. While other examples of C14'-S give a negative CE for this band, analog **25** demonstrates a weak band at 304 nm ($\Delta\varepsilon$ = +3.1). The opposite effect is observed for C14'-R **26** ($\Delta\varepsilon$(303 nm) = -8.6). It appears that the seven-membered ring of these analogs exerts a subtle effect on the vindoline ^1L_b electric transition leading to the difference seen in the CD spectra of **25** and **26**.

Additional analogs: The CD of other vinblastine structural analogs have appeared in the literature. For example, a series of 20'-desethyl-20'-desoxy-vinblastine were prepared and the CD were measured in ethanol.[26] All compounds with C16'-S stereochemistry had positive exciton couplets in the CD spectrum; signs of the ~305 nm CE were also consistent with the analysis of C14' configuration described above.

Theoretical Calculations of the CD of Vinblastine and its Analogs.

Our initial report[18] indicated that the π-SCF-CI-DV molecular orbital CD calculation method[27,28] can be applied to calculate the dipole-dipole interactions between the two chromophores of vinblastine. This calculation also confirmed that the origin of the strong bisignate curve of the vinblastine CD is the exciton coupling between the ^1B_b transitions of the indole and indoline chromophores.

In this study, we describe the CD calculation of vinblastine in a more detailed way and extend this approach to both natural and unnatural analogs of vinblastine at the C16' configuration. The initial step of this CD calculation method requires the conformational analysis of vinblastine (**1**) and its three analogs (**7**, **10**, **11**) in order to obtain energy-minimized structures. It was assumed that the general molecular conformation of vinblastine in solution is similar to that obtained from X-ray crystallography. Since there is no X-ray crystal

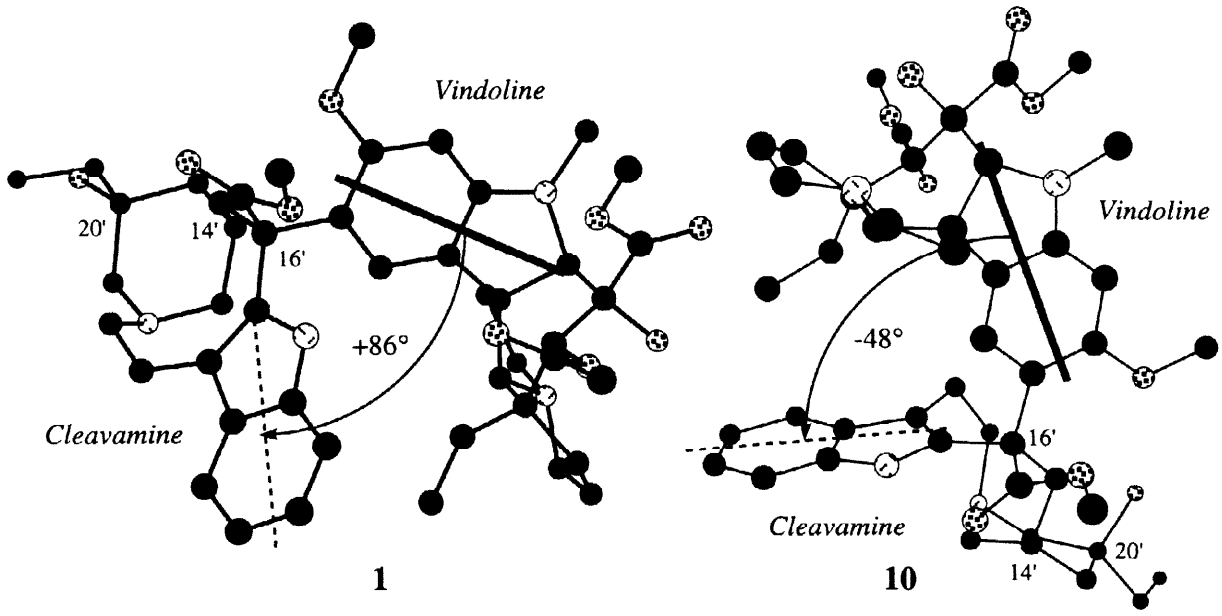

Figure 7. Energy-minimized conformations of vinblastine (**1**) and analog **10**.

structure of vinblastine available, data from vincristine methiodide dihydrate[7] was used as the initial structure for the molecular modeling studies of vinblastine and its analogs. The aldehyde group of vincristine was replaced with a methyl group to obtain initial coordinates for molecular modeling; it was assumed that this substitution would not cause significant conformational changes to the rest of the molecule. Energy minimization with the Amber force field in $CHCl_3$ was utilized to obtain a vinblastine conformation which occupies a local energy minimum (Figure 7).[29] The conformations of vinblastine diastereomers **7**, **10** (Figure 7) and **11** were similarly obtained by inverting the appropriate stereocenter of the vinblastine stereostructure followed by Amber local energy minimization.

The modeling of vindoline (**3**) and cleavamine **4** was performed by using the two half-molecules in the X-ray crystal structure of vincristine after disconnection at C16' as the initial structures for subsequent local energy minimization with the Amber force field.

Assuming that the split CD Cotton effects of vinblastine and its diastereomers were derived from exciton coupling between the indole and indoline chromophores, only the π-π^* transitions of the two chromophores were taken into account for the MO calculations. Because the parameters for the π-electron SCF-CI-DV MO calculation were adjusted to fit the UV spectra of the two separate moieties of vinblastine (**3** and **4**), the UV calculations were initiated from the atomic coordinates obtained from the energy minimizations described above. The following standard values of atomic orbital parameters were used for all the included calculations: for sp^2 carbons, Z(C) = 1.0, W(C) = -11.16 eV, (rr|rr)(C) = 11.13 eV, β(C-C, 1.388 Å) = -2.22 eV, $<\nabla>$(C-C, 1.388 Å) = 4.70×10^7 cm^{-1}; for ether oxygens (sp^3), Z(O) = 2.0, W(O) = -33.00 eV, (rr|rr)(O) = 21.03 eV, β(C-O) = 1.60 eV, $<\nabla>$(C-O) = 5.00×10^7 cm^{-1}. The nitrogen atoms in the indole and indoline chromophores were treated as singly- and doubly-charged species, respectively: for the indole nitrogen (sp^2), Z(N) = 1.0, W(N) = -16.18 eV, (rr|rr)(N) = 11.50 eV, β(C-N) = -2.88 eV, $<\nabla>$(C-N) = 4.10×10^7 cm^{-1}; for the indoline nitrogen (sp^3) Z(N) = 2.0, W(N) = -27.70 eV, (rr|rr)(N) = 19.00 eV, β(C-N) = -1.80 eV, $<\nabla>$(C-N) = 5.70×10^7 cm^{-1}. The electric repulsion integral (rr|ss) was estimated using the Nishimoto-Mataga equation.[30] The resonance integral and del value were calculated by employing the following equations:

$$\beta = [S/S(\text{C-C, 1.388 Å})]\beta(\text{C-C, 1.388 Å}) \cos\theta$$
$$<\nabla> = [<\nabla>(\text{empir, 1.388 Å})/<\nabla>(\text{theor, 1.388 Å})]<\nabla>(\text{theor})\cos\theta$$

where θ is the dihedral angle. The values of the overlap integral S and $<\nabla>$(theor) were calculated based on the Slater orbital. The summation of the component CD and UV bands were approximated by Gaussian distributions

$$\Delta\varepsilon(\sigma) = \Sigma\Delta\varepsilon_k \exp[-((\sigma-\sigma_k)/\Delta\sigma)^2]$$
$$\varepsilon(\sigma) = \Sigma\varepsilon_k \exp[-((\sigma-\sigma_k)/\Delta\sigma)^2]$$

where the standard deviation value $\Delta\sigma$ = 2180 cm^{-1} was obtained as an average of the experimental half band widths of cleavamine and vindoline.

It was assumed that the π-electron systems of the indole and indoline chromophores make the most significant contributions to the electric transition dipole moments, giving rise to the exciton coupled CD. The calculation of the UV spectra of cleavamine and vindoline provided the orientation and dipole strengths of the ^1B_b,

^1L_a, and ^1L_b transitions of the indole and indoline chromophores (Figure 8). The calculated UV spectra of vindoline (**3**) and cleavamine **4** correlate well with the experimental data, both in position of the bands and their intensities (see Figures 9 and 10).

Based on the physical parameters obtained for UV calculations of vindoline (**3**) and cleavamine **4**, the CD and UV spectra of vinblastine and its analogs were calculated (Table 4) considering the interactions between the 70 singly excited states of lowest energy and using the conformation obtained from energy minimization (Figure 7).

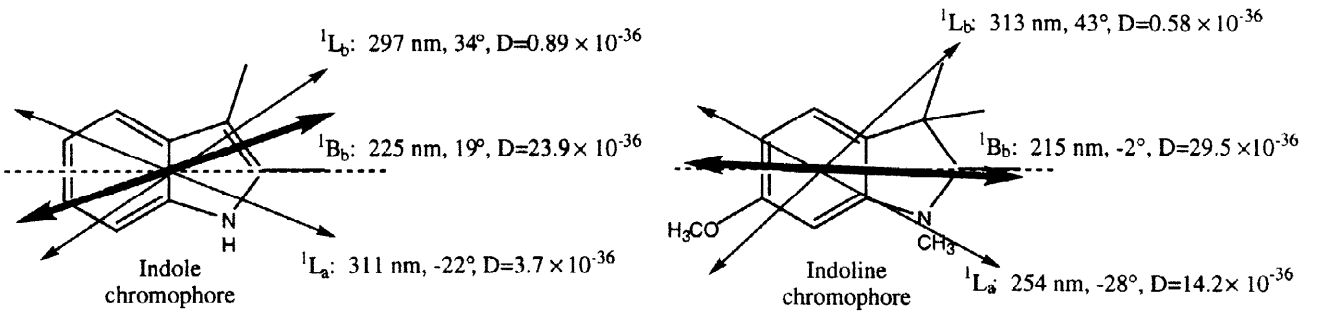

Figure 8. Calculated transition moments of indole and indoline chromophores of vinblastine. The angle indicated for each transition is its relationship with the long axis of the chromophore (dashed line). The strongest transition (^1B_b) is in bold. The dipole strength of each transition is in cgs units.

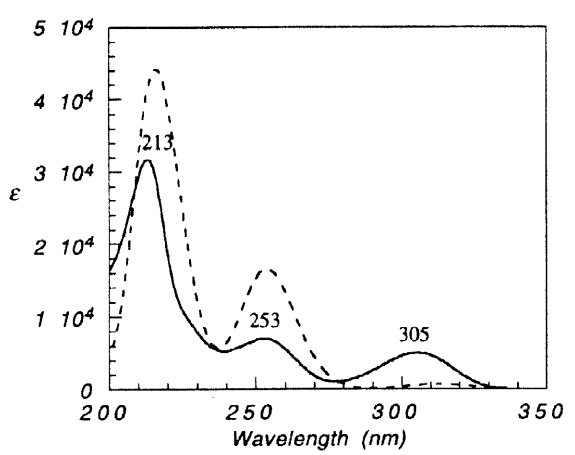

Figure 9. Comparison of experimental (solid line) and calculated (dashed line) UV spectra of vindoline (**3**). λmax for the experimental curve are indicated.

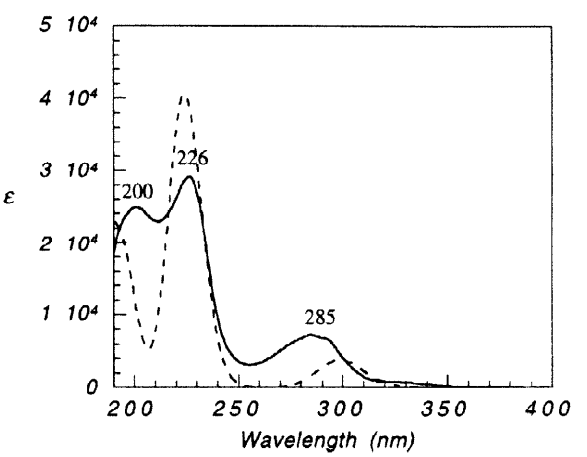

Figure 10. Comparison of experimental (solid line) and calculated (dashed line) UV spectra of cleavamine **4**. λmax for the experimental curve are indicated.

Figure 11 compares the calculated CD spectra of vinblastine with both the experimental data as well as the difference CD described earlier. It is clear that the calculations are able to derive the position, sign, and shape of the exciton couplet, although the intensity of these CEs are weaker than both the experimental and difference CD values. Importantly, the good similarity between observed and calculated split CD bands at 210 - 230 nm confirms the correlation between the positive exciton couplet and C16'-S absolute configuration in vinblastine,

where the projection angle between two ^1B_b transition moment vectors is +86° (Figure 7). The CD and UV calculations of **10** were performed based on its molecular geometry (Figure 7). Following the same procedure that was carried out for vinblastine, the projection angle between the two ^1B_b transition moment vectors of **10** was estimated to be -48°. The opposite C16'-R configuration gives negative couplets in both experimental and calculated CD spectra (Figure 12). In addition, theoretical CD and UV calculations were executed for vinblastine analogs **7** and **11** (Table 4). The calculated CD spectra of **7** and **11** were also able to reveal the appropriate exciton coupled spectra.

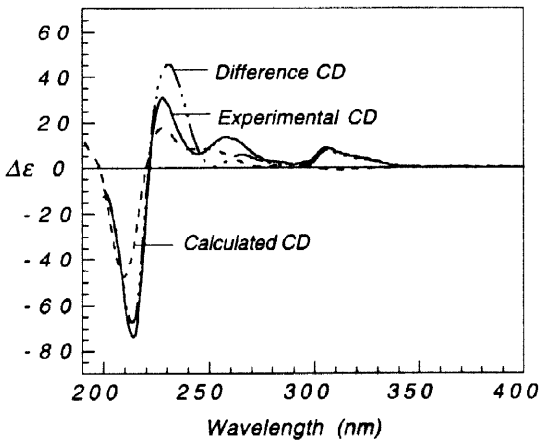

Figure 11. Comparison of calculated, experimental and difference CD spectra of vinblastine (**1**).

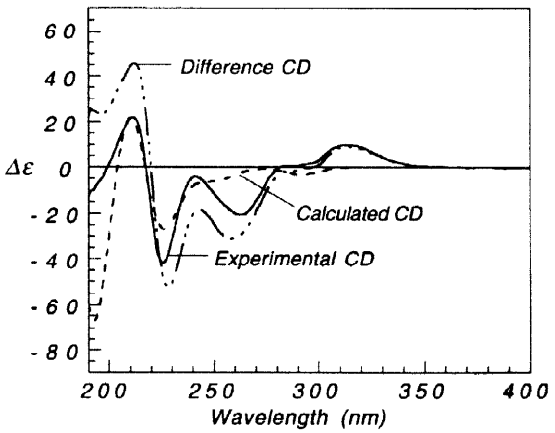

Figure 12. Comparison of calculated, experimental and difference CD spectra of vinblastine analog **10**.

However, the calculation did not provide good agreement in the shape of the CEs at 255 and 310 nm. It is anticipated that the origin of these CEs is due to interactions of electric transitions with the chiral environment which can not be properly evaluated in this calculation method based on the dipole velocity formalism. In this method, the rotational strength arising from dipole-dipole interactions and resulting in an exciton split curve is derived as a function of interchromophoric distance vectors which are origin-independent, while the contributions from the internal magnetic moment of the chromophores are negligible. While this approximation reasonably predicts the exciton coupling of vinblastine and its analogs between 210 and 230 nm, it is unsuitable for the evaluation of other CD bands at longer wavelengths which result from the interaction of electric and magnetic transition dipole moments of the inherently chiral vindoline and cleavamine "half-molecules".

Correlation of stereochemistry with bioactivity.[16,31-33]

It is known that the 16'-S stereochemistry is required for *Vinca* alkaloid binding and inhibition of microtubule polymerization as well as for cytotoxic activity. The 16'-S configuration, however, is not sufficient for the design of bioactive vinblastine analogs.[16,32,33] There is also a strong correlation of bioactivity with 14'-R stereochemistry, but the configuration at the 20'-position is relatively unimportant. Vinblastine (**1**), vincristine (**2**) and leurosidine (**5**) with the 14'-R/16'-S configuration are all active in microtubule polymerization assays and also bring about mitotic arrest in cultured cells; vinblastine (**1**) and leurosidine (**5**) differ only in the configuration at the 20'-position (vinblastine, 20'-S; leurosidine, 20'-R). Vinblastine diastereomers **6-11** with 14'-S/16'-S, 14'-

R/16'-R, and 14'-S/16'-R configurations are not active in either microtubule polymerization or cytotoxicity studies.[16,32,33] As might be expected for a ligand-protein interaction, there is exquisite stereoselectivity for the binding of the *Vinca* alkaloids at their binding site on tubulin. This is further confirmed by the lack of activity of the monomeric vindoline (**3**) or any of the cleavamine diastereomers (**4, 12-18**) in the bioassays.[16,32,33] While it is not surprising that these "half-molecules" (**3** and **4**) do not behave in the same manner as vinblastine itself, it should be noted that vindoline (**3**) is able to modulate the activity of vinblastine when cells are treated with vinblastine and vindoline concurrently.[16] This indicates that vindoline (**3**) is able to bind to the protein, presumably at the same binding site.

While vinblastine analogs **5-12** differ from vinblastine (**1**) only in the configuration at C14', C16' and/or C20', additional vinblastine analogs have been prepared which alter the chemical composition of the molecule more significantly. Epoxides **19-22** which are precursors to the corresponding vinblastine diastereomers (**1, 5, 8** and **9**) have been tested in microtubule polymerization and cytotoxicity assays. In these cases where the piperidine ring is missing, no bioactivity is observed.[16,32,33] However, spiro analog **23** which possesses the 14'-R/16'-S configuration is active in microtubule polymerization assays and is able to elicit mitotic arrest in cultured cells.[31] The results of spiro compound **23** show that the original vinblastine ring system is not necessarily required for bioactivity. However, the C14' and C16' stereochemistry remains critical for this activity since spiro analog **24** with 14'-S/16'-R configuration has no activity. Seven-membered ring analogs **25** and **26** provide some insight into the greater importance of the C16' configuration as compared to C14'. In this case, analog **25** (14'-S/16'-S) is active in the biochemical and cell based assays, but its diastereomer **26** (14'-R/16'-R) is not.[31] While it is the 16'-S configuration which is required for activity, the presence of the C14'-S configuration does not eliminate activity despite the fact that the overall preference for an active analog is C14'-R. It is hypothesized that the larger seven-membered ring in **25** (as compared to the six-membered ring in vinblastine (**1**)) provides enough conformational flexibility so that a productive binding event can occur despite the fact that the C14'-S configuration is less desirable. It would be of interest to obtain bioactivity data on the C14'-epi-**25** with 14'-R/16'-S to determine whether this would lead to even greater activity.

The correlation of activity with C14' and C16' allows for the CD analysis of novel vinblastine analogs in order to determine which compounds have the proper configuration for inhibition of tubulin polymerization. The exciton coupling between the indole and indoline chromophores of vinblastine (**1**) and its analogs allows for a clear determination of the C16' configuration and an indication as to whether a compound should be further analyzed for its bioactivity. At this point, no exception to the rule which correlates C16'-S analogs with a positive 228 nm/214 nm couplet and C16'-R with a negative couplet has been identified. The sign of the CE at 300-310 nm gives an indication of the C14' stereochemistry, but, especially since the origin of this band is not from exciton coupling, it is more sensitive to other modifications of the molecule. All analogs described here have a positive CE when C14' is R and a negative band when C14' is S except for seven-membered ring analogs **25** and **26**. In this case, the trend is reversed in that C14'-S (**25**) has a negative Cotton effect at 304 nm ($\Delta\varepsilon$ = +3.1) and C14'-R (**26**) has a positive Cotton effect at 303 nm ($\Delta\varepsilon$ = -7.8); it is interesting to note that the analog with the positive CE between 300 and 310 nm (**25**), similar to that seen in vinblastine (305 nm, $\Delta\varepsilon$ = +9.0), is also the analog which is bioactive.

CONCLUSION

The CD spectra of a wide variety of vinblastine analogs have confirmed the reliability for determining C16' configuration. Bioactive analogs with the natural C16'-S stereochemistry, without exception, exhibit strong positive exciton coupled CD, while analogs with the unnatural C16'-R stereochemistry lead to strong negative exciton coupled spectra. Since the intense exciton coupling of the indole and indoline chromophore ^1B_b transitions is not sensitive to a wide variety of structural changes, the use of CD to assign the C16' stereochemistry of vinblastine analogs appears to be a general non-empirical method. All bioactive vinblastine analogs have a positive CE at ~305 nm which in all but one example correlates with a C14'-R configuration. The clear connection between the sign and shape of the CD spectrum allows for a preliminary method for the screening of vinblastine analogs with potential bioactivity. Theoretical calculations of the CD spectra of these compounds derive the dipolar interactions which lead to the strong bisignate curve and support the interpretation of these bands as originating from exciton coupling.

EXPERIMENTAL

General.

All calculations of UV and CD spectra and Macromodel energy minimizations were performed on a Indigo Silicon Graphics 3D workstation . ^1H and ^{13}C NMR spectra were recorded on a Bruker AMX-400. Vindoline and vinblastine were generously supplied by Dr. A. J. Hannart of Omnichem. Vincristine was purchased from Fluka. Dichloromethane, acetone, triethylamine, silver tetrafluoroborate, acetonitrile (spectrophotometric grade) and potassium borohydride were purchased from Aldrich Chemical Company. Centrifugal chromatography was performed on a Harrison Chromatotron and used with E. Merck 60 PF-254 silica with gypsum. (+)-Pandoline, (-)-pandoline, 20'-epi-(+)-pandoline and 20'-epi-(-)-pandoline were prepared as previously described.[22,23,34] Vinblastine (**1**), leurosidine (**5**), vincovaline (**8**), 20'-epi-vincovaline (**9**) and epoxides **19-22** were prepared as described previously.[12] Cleavamine diastereomers (**4**, **13-18**) were prepared as described previously.[8,9,22-25] Cleavamine diastereomer **12** was not available for this study. The synthesis of the spiro (**23**, **24**) and seven-membered ring (**25**, **26**) vinblastine analogs was accomplished using similar methodology to that used for the other vinblastine diastereomers[12] and will be described in detail separately. The synthesis of vinblastine diastereomers **6-7** and **10-11** is described below.

UV and CD spectra.

Solutions of known concentration were prepared by measuring the exact weight (Sartorius Ultramicro Balance) of each compound (50-100 μg) in a volumetric flask. Extinction coefficients were determined by averaging the data from three separate samples (pathlength=10 mm). UV spectra were obtained with a Perkin-Elmer Lambda 40 UV-VIS spectrometer. CD spectra were taken in acetonitrile and the concentration of each sample was determined based on extinction coefficients at the respective λmax. Spectra were obtained with a Jasco J-720 spectropolarimeter using a 10 mm cell. Typical parameters: scans, 4; band width, 1.0 nm; scan speed, 100 nm/min; range, 400-190 nm; resolution, 1.0 nm.

Synthesis.

Vinblastine analog **11**. To a solution of 20'-epi-(-)-pandoline (88.4 mg, 0.25 mmol) and triethylamine (52 μL, 0.37 mmol, 1.5 eq) in dichloromethane (20 mL) at 0 °C was added *t*-butyl hypochlorite (436 μL, 0.375 mmol, 1.5 eq). After 15 min, the reaction mixture was washed with iced water (50 mL) and the layers were separated. The aqueous layer was extracted with additional dichloromethane (2 × 25 mL) and the combined organic layers were combined, dried over anhydrous magnesium sulfate and concentrated under reduced pressure to give a deep yellow-orange viscous oil. To the resulting chloroimine dissolved in dry acetone (2.5 mL, freshly distilled from boron oxide) was added vindoline (114 mg, 0.25 mmol, 1 eq) followed by a solution of silver tetrafluoroborate (146 mg, 0.75 mmol, 3 eq) in dry acetone (0.5 mL). After stirring for 30 min at 20 °C, the mixture was poured into 10% ammonium hydroxide saturated with NaCl (10 mL) and extracted with dichloromethane (4 × 10 mL). The combined dichloromethane portions were combined, dried with magnesium sulfate and concentrated under reduced pressure to provide a foam. This residue was immediately taken up in glacial acetic acid (5 mL) and potassium borohydride (135 mg, 2.5 mmol, 20 eq) was added in small portions. The reaction mixture was then transferred to crushed ice (20 mL), basicified with concentrated ammonium hydroxide (ca. 10 mL), and extracted with dichloromethane (20 mL). After separating the two layers, the aqueous layer was extracted with dichloromethane (3 × 10 mL). The combined dichloromethane portions were dried with magnesium sulfate and concentrated under reduced pressure to give a tan foam. This residue was then purified by chromatotron chromatography on a 4 mm silica gel plate at a flow rate of 2.6 mL/min. Fractions were combined and the solvents were removed under reduced pressure to give an off-white foam. An additional chromatotron chromatography with a 2 mm silica gel plate eluting with 10% methanol in dichloromethane at a flow rate of 1.4 mL/min provided the desired product as a white foam (21 mg, 10.4% yield based on vindoline). R_f=0.21 (1:9 methanol:dichloromethane). ^{1}H NMR (400 MHz, $CDCl_3$) δ 0.62 (t, J=7.1 Hz, 3H), 1.00 (t, J=7.3 Hz, 3H), 1.21 (septet, J=7.0, 1H), 1.38 (br d, J=13.4 Hz, 1H), 1.58-1.78 (m, 3H), 1.89-2.22 (m, 4H), 2.08 (s, 3H), 2.48-2.65 (m, 2H), 2.62 (s, 3H), 2.74 (s, 1H), 2.86-3.14 (m, 5H), 3.32-3.61 (m, 7H), 3.68 (s, 1H), 3.76 (s, 6H), 3.88 (s, 3H), 3.82-3.93 (m, 1H), 5.29 (d, J=9.8 Hz, 1H), 5.37 (s, 1H), 5.90 (dd, J=3.8, 9.9 Hz, 1H), 6.00 (s, 1H), 6.90 (s, 1H), 7.02 (t, J=7.0 Hz, 1H), 7.12 (t, J=7.54 Hz, 1H), 7.26 (d, J=7.7 Hz, 1H), 7.39 (d, J=7.8 Hz, 1H), 9.04 (br s, 1H), 9.47 (br s, 1H). ^{13}C (100 MHz, $CDCl_3$) δ 7.28, 7.33, 20.47, 23.90, 30.45, 30.98, 34.50, 37.80, 41.03, 41.59, 42.66, 43.45, 46.16, 50.74, 51.51, 51.65, 52.52, 53.77, 55.64, 59.21, 66.80, 70.52, 76.14, 79.28, 82.92, 94.21, 110.22, 110.36, 117.37, 118.37, 119.32, 121.29, 123.87, 124.65, 125.41, 127.74, 130.05, 133.53, 134.37, 151.90, 156.21, 170.20, 171.32, 174.66.

Vinblastine analog **6**. Coupling of (+)-pandoline was done in the same manner as described above to provide **6** (24.5 mg, 11.1% yield). R_f=0.43 (1:9 methanol:methylene chloride). ^{1}H NMR (400 MHz, $CDCl_3$) δ -0.09 (t, J=7.23 Hz, 3H), 0.61 (septet, J=7.29 Hz, 1H), 0.92 (t, J=7.54 Hz, 3H), 1.31 (septet, J=7.34 Hz, 1H), 1.40-1.47 (m, 2H), 1.58-1.65 (m, 3H), 1.80 (m, 1H), 1.99 (s, 3H), 2.13 (d, J=13.9 Hz, 1H), 2.24-2.58 (m, 6H), 2.64 (s, 3H), 2.79-3.03 (m, 4H), 3.13-3.51 (m, 5H), 3.71 (s, 1H), 3.75 (s, 6H), 3.89 (s, 3H), 4.49 (t, J=12.9 Hz, 1H), 5.05 (d, J=10.1 Hz, 1H), 5.28 (s, 1H), 5.78 (dd, J=3.5, 10.1 Hz, 1H), 6.04 (s, 1H), 6.94 (t, J=7.6 Hz, 1H), 7.06 (t, J=7.5 Hz, 1H), 7.13 (s, 1H), 7.21 (d, J=8.5 Hz, 1H), 7.28 (d, J=7.6 Hz, 1H), 8.91 (s, 1H), 9.63 (s, 1H). ^{13}C NMR (100 MHz, $CDCl_3$) δ 6.85, 6.94, 20.70, 29.92, 30.89, 32.28, 34.15, 38.26, 38.89, 42.79, 43.02, 43.97, 50.19, 51.02, 51.67, 51.82, 52.29, 53.16, 53.44, 54.99, 55.89, 65.72, 67.51, 70.85, 76.44, 79.49, 83.63, 94.55, 110.28, 110.79, 117.82, 118.27, 119.97, 121.25, 123.71, 125.56, 126.54,

128.58, 130.57, 134.76, 134.99, 152.26, 156.44, 170.31, 171.88, 175.32.

16'-epi-Vinblastine (**10**). Coupling of (-)-pandoline was done in the same manner as described above to provide **10** (23.7 mg, 11.1% yield). R_f=0.42 (1:9 methanol:methylene chloride). 1H NMR (400 MHz, CDCl3) δ 0.70 (t, J=7.3 Hz, 3H), 0.90 (t, J=7.4 Hz, 3H), 1.26-1.38 (m, 4H), 1.49-1.66 (m, 7H), 1.92-2.05 (m, 3H), 2.06 (s, 3H), 2.43-2.46 (m, 2H), 2.56-2.68 (m, 1H), 2.82-3.11 (m, 6H), 2.88 (s, 1H), 3.24-3.49 (m, 5H), 3.68 (s, 1H), 3.76 (s, 3H), 3.75 (s, 3H), 3.88 (s, 3H), 4.52 (m, 1H), 5.33 (d, J=10.2 Hz, 1H), 5.34 (s, 1H), 5.94 (dd, J=10.2, 3.7 Hz, 1H), 5.98 (s, 1H), 6.99 (t, J=8.0 Hz, 1H), 7.09 (t, J=7.4 Hz, 1H), 7.24 (d, J=8.0 Hz, 1H), 7.38 (d, J=7.9 Hz, 1H), 9.04 (br s, 1H), 9.67 (br s, 1H). ^{13}C NMR (100 MHz, $CDCl_3$) δ 6.83, 7.63, 21.13, 29.69, 30.64, 32.02, 34.22, 38.25, 39.17, 42.72, 43.76, 50.52, 50.59, 52.00, 52.13, 52.89, 53.27, 55.12, 56.00, 65.19, 70.69, 77.21, 76.47, 94.26, 110.40, 110.54, 117.96, 118.26, 119.83, 121.26, 123.88, 124.58, 126.25, 128.32, 130.44, 131.99, 134.49, 135.36, 151.74, 156.16, 170.84, 171.84, 175.47.

14'-epi-Vinblastine (**7**). Coupling of 20'-epi-(+)-pandoline was done in the same manner as described above to provide **7** (21.8 mg, 10.8% yield). R_f=0.30 (1:9 methanol:methylene chloride). ^{1}H NMR (400 MHz, $CDCl_3$) δ 0.00 (t, J=7.3 Hz, 3H), 0.69 (septet, J=7.7 Hz, 1H), 1.13 (t, J=7.3 Hz, 3H), 1.40 (septet, J=7.1 Hz, 1H), 1.53 (d, J=14.5 Hz, 1H), 1.75 (septet, J=7.3 Hz, 1H), 1.88 (septet, J=6.8 Hz, 1H), 2.02-2.81 (m, 2H), 2.11 (s, 3H), 2.19 (m, 1H), 2.34 (d, J=13.0 Hz, 1H), 2.43-2.47 (m, 2H), 2.56 (s, 1H), 2.60-2.64 (m, 1H), 2.76 (s, 3H), 2.92 (d, J=16.0 Hz, 1H), 2.99-3.08 (m, 2H), 3.11-3.23 (m, 3H), 3.40-3.72 (m, 7H), 3.83 (s, 1H), 3.86 (s, 3H), 3.88 (s, 3H), 4.01 (s, 3H), 5.16 (d, J=10.1 Hz, 1H), 5.30 (s, 1H), 5.88 (dd, J=4.2, 10.2 Hz, 1H), 6.16 (s, 1H), 7.00 (s, 1H), 7.10 (t, J=7.4 Hz, 1H), 7.21 (t, J=7.1 Hz, 1H), 7.34 (d, J=8.0 Hz, 1H), 7.42 (d, J=7.9 Hz, 1H), 8.99 (s, 1H), 9.71 (br s, 1H). ^{13}C NMR (100 MHz, $CDCl_3$) δ 6.87, 7.40, 20.90, 23.50, 30.71, 30.86, 34.79, 38.25, 41.05, 41.28, 42.57, 44.04, 45.55, 50.03, 52.20, 52.28, 52.94, 53.12, 53.38, 53.91, 55.97, 58.29, 66.86, 70.56, 71.11, 76.18, 77.20, 79.31, 83.39, 94.31, 110.45, 110.59, 117.52, 118.69, 119.46, 121.76, 123.89, 125.10, 125.27, 127.95, 130.22, 132.34, 134.64, 152.26, 156.09, 170.55, 171.77, 174.92.

ACKNOWLEDGEMENTS

This work was supported by NIH grant GM 34509 (K.N.) and an NIH NRSA postdoctoral fellowship to C.A.P. We acknowledge Dr. Tatsuo Nehira for his assistance with the theoretical CD and UV calculations and Dr. Barry Rickman for some CD and UV measurements.

REFERENCES

1. Noble, R. L.; Beer, C. T.; Cutts, J. H. *Ann. N. Y. Acad. Sci.* **1958,** *76*, 882.
2. Svoboda, G. H. *J. Pharm. Sci.* **1958,** *47*, 834.
3. Palmer, C. G.; Livengood, D.; Warren, A. K.; Simpson, R. J.; Johnson, I. S. *Exp. Cell Res.* **1960,** *20*, 198-201.
4. Bensch, K. G.; Malawista, S. E. *J. Cell Biol.* **1969,** *40*, 95-107.
5. Shelanski, M. L.; Wisniewski, J. *Arch. Neurol.* **1969,** *20*, 199-206.
6. Hamel, E. Interaction of tubulin with small ligands. In *Microtubule proteins;* Avila, J. Ed.; CRC Press: Boca Raton, FL, 1990; pp. 89-191.

7. Moncrief, J. W.; Lipscomb, W. N. *Acta Cryst.* **1966,** *21*, 322-331.
8. Wenkert, E.; Cochran, D. W.; Hagaman, E. W.; Schell, F. M.; Neuss, N.; Katner, A. S.; Potier, P.; Kan, C.; Plat, M.; Koch, M.; Mehri, H.; Poisson, J.; Kunesch, N.; Rolland, Y. *J. Am. Chem. Soc.* **1973,** *95*, 4990-4995.
9. Wenkert, E.; Hagaman, E. W.; Kunesch, N.; Wang, N.; Zsadon, B. *Helv. Chim. Acta* **1976,** *59*, 2711-2723.
10. Potier, P.; Langlois, N.; Langlois, Y.; Guéritte, F. *J.C.S Chem. Comm.* **1975**, 670-671.
11. Pearce, H. L. Medicinal chemistry of bisindole alkaloids from *Catharanthus*. In *The Alkaloids;* Brossi, A.; Suffness, M. Eds.; Academic Press: San Diego, CA, 1990; Vol. 37; pp. 145-204.
12. Kuehne, M. E.; Matson, P. A.; Bornmann, W. G. *J. Org. Chem.* **1991,** *56*, 513-528.
13. Potier, P. *J. Nat. Prod.* **1980,** *43*, 72-86.
14. Kuehne, M. E.; Marko, I. Synthesis of Vinblastine-Type Alkaloids. In *The Alkaloids;* Brossi, A.; Suffness, M. Eds.; Academic Press: New York, 1990; Vol. 37; pp. 77-131.
15. Borman, L. S.; Kuehne, M. E. Functional hot spot at the C-20' position of vinblastine. In *The Alkaloids;* Brossi, A.; Suffness, M. Eds.; Academic Press: San Diego, 1990; Vol. 37; pp. 133-144.
16. Borman, L. S.; Bornmann, W. G.; Kuehne, M. E. *Cancer Chemother. Pharmacol.* **1993,** *31*, 343-349.
17. Kutney, J. P.; Gregonis, D. E.; Imhof, R.; Itoh, I.; Jahngen, E.; Scott, A. I.; Chan, W. K. *J. Am. Chem. Soc.* **1975,** *97*, 5013-5015.
18. Dong, J.-G.; Bornmann, W.; Nakanishi, K.; Berova, N. *Phytochemistry* **1995,** *40*, 1821-1824.
19. Langois, N.; Guéritte, F.; Langlois, Y.; Potier, P. *J. Am. Chem. Soc.* **1976,** *98*, 7017-7024.
20. Albinsson, B.; Kubista, M.; Thulstrup, E.; Norden, B. *J. Phys. Chem.* **1989,** *93*, 6646.
21. Albinsson, B.; Norden, B. *J. Phys. Chem.* **1992,** *96*, 6204.
22. Kuehne, M. E.; Kirkemo, C. L.; Matsko, T. H.; Bohnert, J. C. *J. Org. Chem.* **1980,** *45*, 3259-3265.
23. Bruneton, J.; Cavé, A.; Hagaman, E. W.; Kunesch, N.; Wenkert, E. *Tetrahedron Lett.* **1976**, 3567-3570.
24. Kunesch, N.; Vaucamps, P.-L.; Cavé, A.; Poisson, J. *Tetrahedron Lett.* **1979**, 5073-5076.
25. Le Men, J.; Hugel, G.; Zeches, M.; Hoizey, M.-J.; Le Men-Olivier, L.; Lévy, J. *C. R. Acad. Sci. Paris, Ser. C* **1976,** *283*, 759-761.
26. Kuehne, M. E.; Zebovitz, T. C.; Bornmann, W. G.; Marko, I. *J. Org. Chem.* **1987,** *52*, 4340-4349.
27. Harada, N.; Uda, H.; Kobayashi, M.; Shimizu, N.; Kitagawa, I. *J. Am. Chem. Soc.* **1989,** *111*, 5668.
28. Harada, N.; Nakanishi, K. Circular Dichroic Spectroscopy-Exciton Coupling in Organic Stereochemistry; University Science Books: Mill Valley, CA, 1983.
29. Still, W. C.; Tempczyk, A.; Hawley, R. C.; Hendrickson, T. *J. Am. Chem. Soc.* **1990,** *112*, 6127.
30. Nishimoto, K.; Mataga, N. *Z. Physik. Chem.* **1957,** *12*, 335.
31. Bornmann, W. G.; Kuehne, M. E.; Borman, L. S. "Total synthesis of four vinblastine congeners and their biochemical evaluation"; 22nd National Mecicinal Chemistry Symposium, 1990, Austin, TX.
32. Borman, L. S.; Kuehne, M. E.; Matson, P. A.; Marko, I.; Zebovitz, T. C. *J. Biol. Chem.* **1988,** *263*, 6945-6948.
33. Borman, L. S.; Kuehne, M. E. *Biochem. Pharm.* **1989,** *38*, 715-724.
34. Zeches, M.; Debray, M.-M.; Ledouble, G.; Le Men-Olivier, L.; Le Men, J. *Phytochemistry* **1975,** *14*, 1122-1124.